agronomy

MDPI

Article

Silicate Agrominerals Mitigate Greenhouse Gas Emissions and Enhance Soil Carbon in Tropical Pasture of the Brazilian Cerrado

Marcos Vinícius Araujo dos Santos [1], Alexsandra Duarte de Oliveira [1,*], Cícero Célio de Figueiredo [2], João Paulo Guimarães Soares [1], Giuliano Marchi [1], Thayná Xavier Santana [2], Altair César Moreira de Andrade [1], Daphne Heloísa de Freitas Muniz [1], José Ferreira Lustosa Filho [2], Arminda Moreira de Carvalho [1], Marcos Aurélio Carolino de Sá [1] and Éder de Souza Martins [1]

[1] Empresa Brasileira de Pesquisa Agropecuária, EMBRAPA Cerrados, Brasilia 73310-970, Brazil; markosvinicius.77@gmail.com (M.V.A.d.S.); jp.soares@embrapa.br (J.P.G.S.); giuliano.marchi@embrapa.br (G.M.); altairmoreira2016@gmail.com (A.C.M.d.A.); daphne.muniz@embrapa.br (D.H.d.F.M.); arminda.carvalho@embrapa.br (A.M.d.C.); marcos.sa@embrapa.br (M.A.C.d.S.); eder.martins@embrapa.br (É.d.S.M.)

[2] Faculty of Agronomy and Veterinary Medicine, University of Brasilia, Campus Darcy Ribeiro, Brasilia 70910-970, Brazil; cicerocf@unb.br (C.C.d.F.); thaynax45@gmail.com (T.X.S.); filhoze04@hotmail.com (J.F.L.F.)

* Correspondence: alexsandra.duarte@embrapa.br; Tel.: +55-61-981355961

Abstract

The mitigation of greenhouse gas emissions in livestock farming is one of the main challenges for agriculture in the Cerrado biome. Among promising practices, the use of soil remineralizers (REM) stands out as a sustainable and complementary alternative to conventional fertilizers. This study evaluated the effects of applying REM derived from basalt and biotite schist on emissions of N_2O, CO_2 and CH_4, the global warming potential (GWP), as well as on soil carbon and nitrogen in *Urochloa brizantha* cv. BRS Paiaguás pasture. The experiment was conducted in randomized blocks with five treatments (control, KCl, basalt 8.33 Mg ha^{-1}, basalt 40 Mg ha^{-1}, and biotite schist 151 Mg ha^{-1}). Results indicated that KCl and high-dose basalt (40 Mg ha^{-1}) promoted greater accumulated N_2O emissions and higher GWP values. In contrast, biotite schist reduced N_2O emissions and showed the lowest GWP (81.67 kg CO_2 eq. ha^{-1}), while basalt at a moderate dose (8.33 Mg ha^{-1}) increased soil C and N stocks. It is concluded that soil remineralizers, especially those derived from biotite schist, represent viable alternatives to reduce environmental impacts and promote the sustainability of tropical agricultural systems in Cerrado biome.

Keywords: silicate agrominerals; greenhouse gas emissions; β–glucosidase; arylsulfatase; low-carbon agriculture; tropical savannas

Academic Editors: Risely Ferraz Almeida, Roberta Camargos de Oliveira and Teodor Rusu

Received: 8 December 2025
Revised: 28 December 2025
Accepted: 4 January 2026
Published: 6 January 2026

1. Introduction

As climate change intensifies, adopting agricultural practices that reconcile ecosystem protection with productive efficiency is increasingly urgent [1,2]. Such practices should enhance carbon capture and storage while maintaining soil health and biodiversity [3]. On the other hand, food systems are responsible for one-third of global greenhouse gas (GHG) emissions [4]. In tropical conditions, the contribution of food systems for GHG is higher and associated mainly with methane emissions [5]. In Brazil, food systems are the leading source of GHG emissions, accounting for about 1.8 GtCO_2e in 2021, or 73.7% of the country's total (2.4 GtCO_2e). Land use change and forestry, driven mainly by deforestation,

accounted for 56.3% (1.0 $GtCO_2e$), while agriculture contributed 33.7% (600.8 $MtCO_2e$) [6]. Cultivated pastures are the predominant land use within Brazilian agribusiness, covering approximately 179 million hectares [7].

Tropical forage grasses, particularly those belonging to the genus *Urochloa* spp. (formerly *Brachiaria* spp.), are especially prominent. Modern tropical livestock systems face the challenge of mitigating their GHG emissions, which in Brazil are driven mainly by enteric fermentation (CH_4) [8,9], and by the use of soluble nitrogen fertilizers (N_2O) [10]. Therefore, strategies that modify soil biogeochemistry to enhance C sequestration and reduce GHG emissions are crucial in tropical regions [11]. In this context, silicate agrominerals (ASi) emerge as a promising tool, acting beyond plant nutrition by directly participating in elemental geochemical cycles [12]. Furthermore, cultivation of Brachiaria enhances soil C sequestration and is an effective strategy for reducing GHG emissions in agricultural systems [13,14].

This scenario highlights the need for comprehensive mitigation measures, strict deforestation controls [15], and agricultural practices [16]. Key actions include integrated pasture management, adoption of low-GHG production systems, and optimization of input use, especially improving fertilizer efficiency [17]. Implementing these measures is essential to align Brazil's agri-food production with its Paris Agreement commitments and to advance global climate mitigation goals [18].

One promising approach is using soil remineralizers (REM), derived from silicate agrominerals (ASi) rock powders that slowly release essential nutrients (K, Ca, Mg) and sustainably enhance soil fertility [19,20]. Therefore, the use of REM should be regarded not merely as an alternative source of nutrients, but as a comprehensive management strategy that supports low-carbon agricultural initiatives, facilitates the restoration of degraded land, and reduces the agricultural sector's reliance on external inputs [21,22]. Long-term research in real-world conditions is still necessary to understand how these factors affect soil carbon levels, aggregate stability, and nutrient efficiency across different tropical regions [20,23–25]. Evidence indicates that basalt-derived REMs reduce soil N emissions, particularly under temperate conditions [26,27], but may offer broader global benefits [28]. Although REMs can enhance soil fertility [29] and promote CO_2 sequestration via accelerated weathering [30], crucial information is still lacking on their direct impact on GHG emissions in tropical pasture systems.

We hypothesized that the application of silicate soil remineralizers in tropical pastures of the Cerrado reduces greenhouse gas emissions and enhances soil carbon and nitrogen stocks compared to conventional K fertilization, with responses depending on the mineral source and application rate. This study evaluated how soil remineralizers applications affect greenhouse gas emissions, global warming potential, environmental drivers, and soil carbon in *Urochloa brizantha* cv. BRS Paiaguás under Cerrado conditions.

2. Materials and Methods

2.1. Site Description and Soil Characterization

The experiment took place at the Embrapa Cerrados experimental field (Figure 1), located in Planaltina, Federal District, Brazil, at coordinates 15°33′33.99″ S, 47°44′12.32″ W, and an altitude of 1035 m. According to the Köppen–Geiger classification, the prevailing climate of the region is designated as type Aw, which features dry winters and a summer rainy season [31]. Between 1974 and 2024, the region received an average of 1336.8 mm of rainfall each year, while the mean temperature during this period was 21.9 °C (Figure 2).

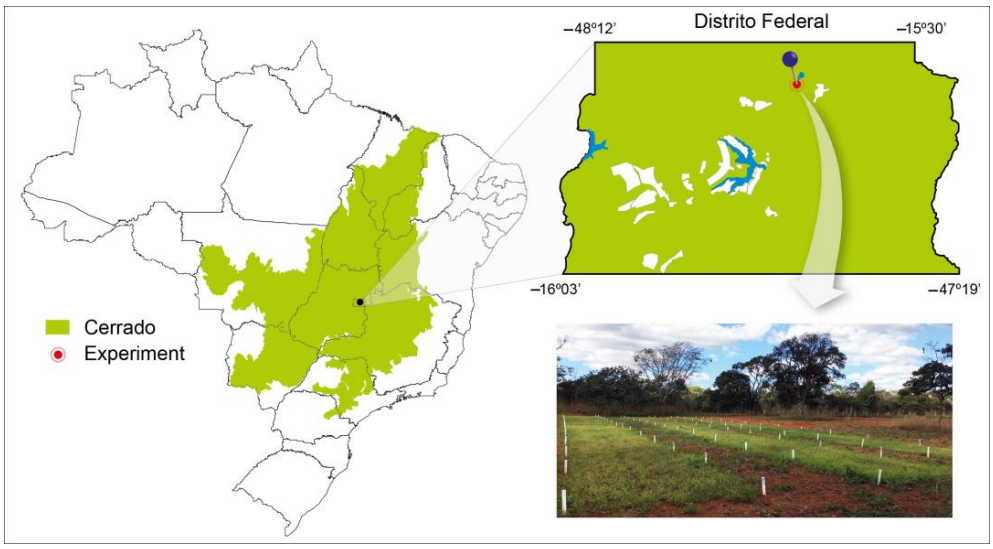

Figure 1. Map of the experimental area of Embrapa Cerrados, Planaltina, Distrito Federal, Brazil.

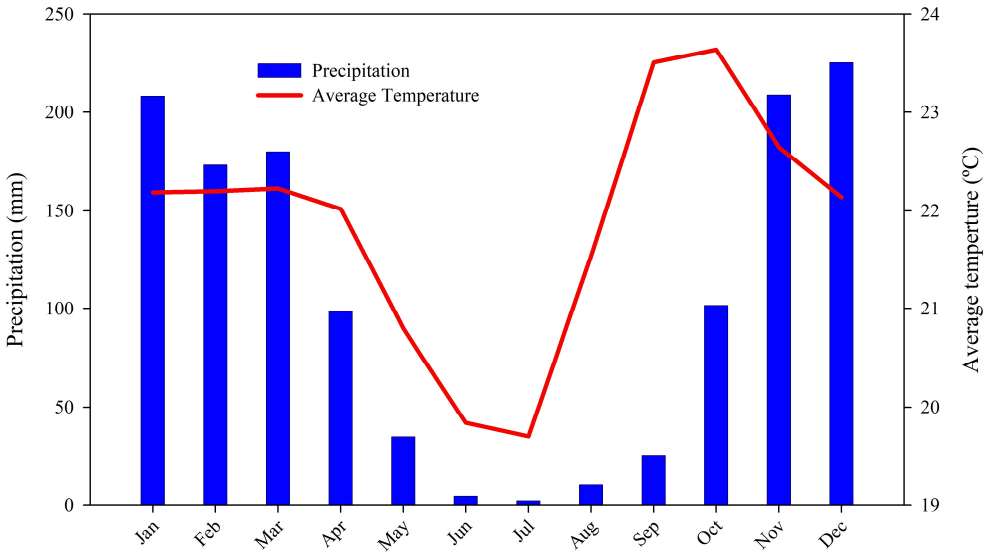

Figure 2. Monthly average rainfall (mm month^{-1}) and temperature (°C) in Planaltina, Distrito Federal, Brazil, from 1974 to 2024.

The soil was identified as a dystrophic Red–Yellow Latosol [32,33] or Ferralsol—FR [34] with a clayey texture. The chemical and physical properties of the soil were determined using the methods described by [35] and are shown in Table 1. In summary, the pH (H_2O) was measured in water at a ratio of 1:2.5 (*v*:*v*) by potentiometry. Ca^{2+}, Mg^{2+}, and Al^{3+} were extracted with 1 mol L^{-1} KCl. Ca^{2+} and Mg^{2+} were measured by atomic absorption spectrometry, and Al^{3+} by volumetry. Available K and P were extracted using the Mehlich-1 method. K^+ was determined by flame photometry, and P was measured with both a flame spectrophotometer and UV–Vis spectrophotometry. H + Al was extracted with 0.5 mol L^{-1} calcium acetate at pH 7 and quantified by alkalimetric titration. Remaining P (P-rem) was determined in solution after stirring 60 mg L^{-1} of P in $CaCl_2$ 10 mmol L for 1 h in a soil:solution ratio of 1:10 [36]. Soil organic carbon (SOC) was assessed via wet oxidation according to [37]. Based on these determinations, we calculated the sum of bases (SB = Ca^{2+} + Mg^{2+} + K^+), the effective cation exchange capacity (effective CEC = Ca^{2+} + Mg^{2+} + K^+ + Al^{3+}), and the cation exchange capacity at pH 7.0 (CEC_{pH7} = Ca^{2+} + Mg^{2+} + K^+ + (H + Al)). Base saturation (BS)

was expressed as [(Ca^{2+} + Mg^{2+} + K^+ + Na^+)/CECpH7] × 100, and Al saturation (m) was calculated as (Al^{3+}/effective CEC) × 100.

Table 1. Baseline chemical characteristics of the soil within the experimental site.

pH H_2O	K^+	Ca^{2+}	Mg^{2+}	Al^{3+}	H + Al	P_{Meh}	OM	TEB	Effective CEC	Total CEC	V	m
	$cmol_c\ dm^{-3}$					$mg\ L^{-1}$	%	$cmol_c\ dm^{-3}$			%	%
5.63	0.06	2.06	0.83	0.01	4.10	0.23	2.87	2.98	2.99	7.09	42.13	0.33

OM = organic matter; TEB = total exchangeable bases; CEC = cation exchange capacity.

2.2. Experimental Design

The long-term experiment was established in September 2015. The design adopted was randomized blocks, with three replications and 14 treatments, and plots measuring 9 m^2 (3 × 3 m). The study tested two REM derived from basalt (BAS) (Serra Geral Group, Araguari, Minas Gerais, Brazil) and from biotite schist (BSC) (Araxá Group, unit B, from Abadiânia, Goiás, Brazil; see [38], for details) as well as two control groups: one using conventional agricultural fertilizer (KCl), and included two controls: a conventional fertilizer treatment (KCl) and an unfertilized K control. All treatments received the same phosphorus fertilization and lime application. For this study, five treatments were selected, resulting in a total of 15 experimental units. The treatments assessed included: T1—a fertilized control without potassium application; T2—a fertilized control with 0.17 t ha^{-1} of KCl; T3—BAS at 8.33 t ha^{-1}; T4—BAS at 40 t ha^{-1}; and T5—BSC at 151 t ha^{-1}.

To adjust soil pH, 500 kg ha^{-1} of dolomitic limestone and 1000 kg ha^{-1} of agricultural gypsum were broadcast and subsequently incorporated into the soil to a depth of 20 cm using a leveling harrow. To address soil fertility requirements, the experimental units were amended with 120 kg ha^{-1} of P_2O_5, supplied as magnesium thermophosphate, along with 100 kg ha^{-1} of FTE BR12, a micronutrient source containing 3.9% sulfur, 1.8% boron, 2.0% manganese, and 9.0% zinc. Once these procedures were finished, each plot received its designated treatment dose, which was applied manually and then mixed into the top 10 cm of soil using a rotary hoe tiller.

Urochloa brizantha cv. BRS Paiaguás was sown on January 25 at an application rate of 3 kg ha^{-1} of viable pure seeds per hectare. The pasture was maintained without grazing throughout the experiment. Nitrogen (as ammonium sulfate, 20% N) was applied at 50 kg ha^{-1}, thirty days after sowing. The plots were maintained in undisturbed, ungrazed condition throughout the experiment, which spanned from 2016 to 2023. During this period, biomass was cut annually during the rainy season. After harvesting, the biomass was removed from the plots to promote regrowth and simulate the effects of grazing.

2.3. Sampling and Analysis of Greenhouse Gas Fluxes

Greenhouse gas flux measurements for CO_2, N_2O, and CH_4 were collected from August 2024 through January 2025. To ensure temporal representativeness, greenhouse gas samples were collected under varying soil moisture conditions, including drought, transition, and rainfall periods. The determination of GHG fluxes was conducted using the static chamber method [39–41].

Each experimental unit was equipped with a chamber. The chamber featured a metal base (measuring 0.38 m by 0.58 m) embedded in the ground and a PVC top section, which was covered with an aluminum thermal blanket. Together, the metal base and PVC upper part sealed off the chamber, creating a microenvironment where gases could accumulate for subsequent collection and analysis using gas chromatography.

Silicone was used to seal central holes in the chambers, allowing insertion of a rubber hose fitted with a three-way valve to regulate gas outflow. A digital thermometer was

installed in one of the chambers to monitor the air temperature inside. A second digital thermometer measured the soil temperature of 5 cm below the surface during the scheduled gas collection times. Gas samples were collected from 9:00 a.m. to 11:00 a.m., capturing the typical daily emission conditions [42].

Gas samples (30 mL each) were collected using 60 mL polypropylene syringes equipped with a three-way valve, then transferred into pre-evacuated vials. Atmospheric air samples were collected from each plot to serve as a reference for the laboratory analysis of gas specimens. The vials were first carried in ice-filled coolers, then placed in refrigerated storage at 18 °C for later reading.

Gas concentrations were measured by gas chromatography with a Nexis GC-2030 (Shimadzu, Kyoto, Japan) equipped with a 30 m × 0.53 mm × 20 µm Rt-QS-BOND capillary column (Restek). Nitrous oxide (N_2O) was measured with an electron capture detector (ECD), and methane (CH_4) and carbon dioxide (CO_2) concentrations were determined using a flame ionization detector (FID) (Shimadzu, Kyoto, Japan).

For analytical precision, the system was calibrated using certified gaseous standards from Messer, Bad Soden, Germany, consisting of defined mixtures diluted in high-purity nitrogen (N_2). Calibration was performed using the following concentration ranges (±standard deviation): N_2O at 0.2 (±0.0), 0.5 (±0.001), 1.0 (±0.1), and 2.0 (±0.1) µmol mol^{-1}; CH_4 at 1.0 (±0.0), 10 (±0.1), 50 (±0.1), and 100 (±0.1) µmol mol^{-1}; and CO_2 at 200 (±0.1), 500 (±0.5), 1000 (±0.8), and 2000 (±2.5) µmol mol^{-1}. The calibration curves demonstrated excellent fit, as indicated by coefficients of determination (R^2) exceeding 0.99.

The quantification limits were estimated to range from 0.08 to 0.13 µmol mol^{-1} for N_2O, from 0.51 to 2.55 µmol mol^{-1} for CH_4, and from 0.60 to 2.88 µmol mol^{-1} for CO_2. Detection limits were found to be between 0.03 and 0.04 µmol mol^{-1} for N_2O, 0.17 to 0.84 µmol mol^{-1} for CH_4, and 0.20 to 0.95 µmol mol^{-1} for CO_2. Based on the sampling time, gas fluxes were determined from these data, and cumulative emissions were estimated through linear interpolation [10].

The fluxes were measured by the linear variation in gas concentration in relation to the incubation time in the sampling chambers, and calculated by Equation (1), as proposed by [43]:

$$FGHG = (\delta C/\delta t) \times (V/A) \times (m/Vm) \quad (1)$$

where FN_2O is the N flow in the form of N_2O (µg N-N_2O m^{-2} h^{-1}); CH_4 (µg C-CH_4 m^{-2} h^{-1}) and CO_2 (mg C-CO_2 m^{-2} h^{-1}) $\delta C/\delta t$ is the slope of the gas concentration curve during the incubation time interval, in nmol/h × L (air); V and A are, respectively, the chamber volume and the soil area covered by the chamber (m^2); m is the molecular weight of N_2O and Vm is the molar volume of the gas at the sampling temperature.

The variables mean air temperature and rainfall were recorded by an automatic weather station (Campbell Scientific) installed next to the experimental area. Soil bulk density (BD) and particle density (PD) were also measured in the plots using volumetric cylinders and a volumetric flask, respectively. Gravimetric soil moisture was determined for a soil subsample by oven-drying at 105 °C for 48 h. Based on the results of soil moisture, BD and PD, the water-filled pore space (WFPS%) at each evaluation was calculated to determine the level of anoxia in the 0–10 cm layer, by Equation (2):

$$WFPS = (\theta \times (BD/WD) \times 100)/[1 - (BD/PD)] \quad (2)$$

where WFPS is the water-filled pore space (%); θ gravimetric water content (g g^{-1}); BD bulk density (g cm^{-3}); WD water density (1.0 g cm^{-3}); and PD particle density (2.65 g cm^{-3}).

The global warming potential (GWP) of GHG emissions, based on a 100-year horizon and Intergovernmental Panel on Climate Change (IPCC) guidelines, was estimated by the following Equation (3):

$$\text{GWP } (\text{kgCO}_2 \text{ eq. ha}^{-1}) = 265 \times \text{cumulative } \text{N}_2\text{O } (\text{kg ha}^{-1}) + 28 \times \text{cumulative } \text{CH}_4 \ (\text{kg ha}^{-1}) \quad (3)$$

2.4. Assessment of Total Soil Carbon

Soil samples were collected on 30 October 2024, at depths of 0–10, 10–20, 20–30, 30–40, and 40–60 cm using a Dutch-type auger. In each plot, a composite sample was prepared at each depth by combining five subsamples. A total of 75 composite samples were collected, representing five treatments, five soil depths, and three replications across three blocks. Soil density was measured using the volumetric ring method [44] at the same depths as C sampling.

The samples were homogenized, transferred to open plastic bags, and air-dried at ambient laboratory temperature. After drying, the material was sieved to <2 mm to obtain Fine Air-Dry Earth (FADE), which was then used for total carbon (TC) determination. For this analysis, subsamples were ground with a mortar and pestle and sieved again to <150 µm.

Soil total carbon (TC) and total nitrogen (TN) concentrations were simultaneously measured via dry combustion using the Vario Macro Cube elemental analyzer (Elementar Analysensysteme, Langenselbold, Germany). Total carbon content was measured via dry combustion using a 2400 Series II CHNS elemental analyzer through high-temperature oxidation at 1000 °C. Carbon and nitrogen stocks were calculated using the equivalent layer method, as outlined in the equations below. To calculate C stock, the C concentrations for each sampled layer were converted into carbon stock values [45].

$$\text{Carbon stock} = (\text{TC} \times \text{BD} - \text{d})/10$$

where TC denotes total soil Carbon (g kg^{-1}), BD represents bulk density (g cm^{-3}), and d refers to the thickness of the soil layer (cm). The value 10 serves as the conversion factor for expressing results in Mg ha^{-1}.

$$\text{Nitrogen stock} = (\text{TN} \times \text{BD} \times \text{d})/10$$

where TN represents total soil nitrogen (g kg^{-1}); BD denotes soil bulk density (g cm^{-3}); d indicates the thickness of the soil layer (cm); and 10 serves as the conversion factor to yield values in Mg ha^{-1}.

2.5. Soil Enzymes

The activities of arylsulfatase and β-glucosidase were determined using a colorimetric method based on p-nitrophenol (PNP) quantification following enzymatic hydrolysis of specific substrates [46] and adapted in recent studies [47]. Air-dried soil samples were sieved through 2 mm mesh and incubated with buffered substrate solutions at 37 °C for 1 h. β-glucosidase activity was measured using p-nitrophenyl-β-D-glucopyranoside as substrate, while arylsulfatase activity was measured using p-nitrophenyl sulfate. After incubation, reactions were terminated with 0.5 M CaCl_2 and 0.1 M NaOH, and PNP absorbance was measured spectrophotometrically using a UV-1800 spectrophotometer (Shimadzu, Kyoto, Japan) at 410 nm for arylsulfatase and 420 nm for β-glucosidase. Enzyme activities were expressed as mg PNP kg^{-1} h^{-1} dry soil. This method is widely employed to assess microbial functional activity related to sulfur and C cycling in soil ecosystems under various land use and management conditions [48].

2.6. Statistical Analysis

Normality and homoscedasticity of the residuals were assessed using the Shapiro–Wilk test. Upon confirming a normal distribution, the data were subjected to analysis of variance (ANOVA), and mean comparisons were performed using Fisher's LSD test ($p < 0.05$) using XLSTAT software 2014.5.03.

3. Results

3.1. Daily Emissions of N_2O, CO_2, and CH_4 and Associated Environmental Variables

The results cover a six-month span, including both the dry season (August–September) and the rainy season (October–January), with weekly frequency. During the assessment period from 30 July 2024 to 22 January 2025, the mean air temperature was recorded at 22.58 °C, with total precipitation reaching 898.8 mm (Figure 3a), and an average relative humidity of 65.17%.

During the evaluation period, daily average N_2O emissions varied among treatments, ranging from −0.13 μg m^{-2} h^{-1} in BSC applied at 151 Mg ha^{-1} to 35.50 μg m^{-2} h^{-1} in the KCl treatment (0.17 Mg ha^{-1}). Intermediate values were observed for BAS, with emissions of 13.41 μg m^{-2} h^{-1} at 8.33 Mg ha^{-1} and 33.47 μg m^{-2} h^{-1} at 40 Mg ha^{-1}, while the control treatment showed an average emission of 9.55 μg m^{-2} h^{-1}. Typically, N_2O emissions differ noticeably between dry and rainy seasons. The greatest N_2O emission recorded during the study was 326.87 μg m^{-2} h^{-1}, observed in November 2024 under the BAS at 40 Mg ha^{-1} treatment, which had an WFPS of 76.75%. The minimum N_2O emission rate, recorded at −162.61 μg m^{-2} h^{-1}, occurred during the rainy season for BSC applied at 8.33 Mg ha^{-1}, with an WFPS < 50% (Figure 3a,b,e).

Following the initial rainfall events, a significant increase in CO_2 emissions was observed, consistent with the pattern observed for N_2O. On 21 January 2025, the BAS 8.33 Mg ha^{-1} treatment exhibited the highest emission peak, achieving a value of 281.32 m^{-2} h^{-1} and an WFPS of 68% (Figure 3a,c,e).

The average daily methane (CH_4) emissions for the respective treatments were as follows: BAS at 8.33 Mg ha^{-1}, 12.45 μg m^{-2} h^{-1}; BAS at 40 Mg ha^{-1}, 4.65 μg m^{-2} h^{-1}; BSC at 151 Mg ha^{-1}, 3.27 μg m^{-2} h^{-1}; KCl at 0.17 Mg ha^{-1}, 13.41 μg m^{-2} h^{-1}; and Control, −14.98 μg m^{-2} h^{-1}. Methane (CH_4) emissions varied between −58.18 μg m^{-2} h^{-1} and 123.45 μg m^{-2} h^{-1} throughout the evaluation period. The lowest emission, 66.6 μg m^{-2} h^{-1} (WFPS 19.84%), was recorded with KCl at 0.17 Mg ha^{-1} during the dry period, while the highest, 123.45 μg m^{-2} h^{-1}, occurred with BAS at 40 Mg ha^{-1} during heavy rainfall (Figure 3a,d,e).

The average nitrate (NO_3^-) content measured in the soil was 0.56 mg kg^{-1} for both the BAS at 8.33 Mg ha^{-1} and BAS at 40 Mg ha^{-1} treatments, 0.55 mg kg^{-1} for BSC at 151 Mg ha^{-1}, 0.54 mg kg^{-1} for KCl 0.17 Mg ha^{-1}, and 0.53 mg kg^{-1} in the Control group (Table 2). The average concentrations of ammonium (NH_4^+) were 5.76, 6.30, 5.14, 5.12, and 4.84 mg kg^{-1}, corresponding to the respective treatment order. During the evaluation period, the mean soil temperatures were 23.07 °C for BAS at 8.33 Mg ha^{-1}, 23.64 °C for BAS at 40 Mg ha^{-1}, 23.89 °C for BSC at 151 Mg ha^{-1}, 23.73 °C for KCl at 0.17 Mg ha^{-1}, and 23.73 °C for the Control treatment.

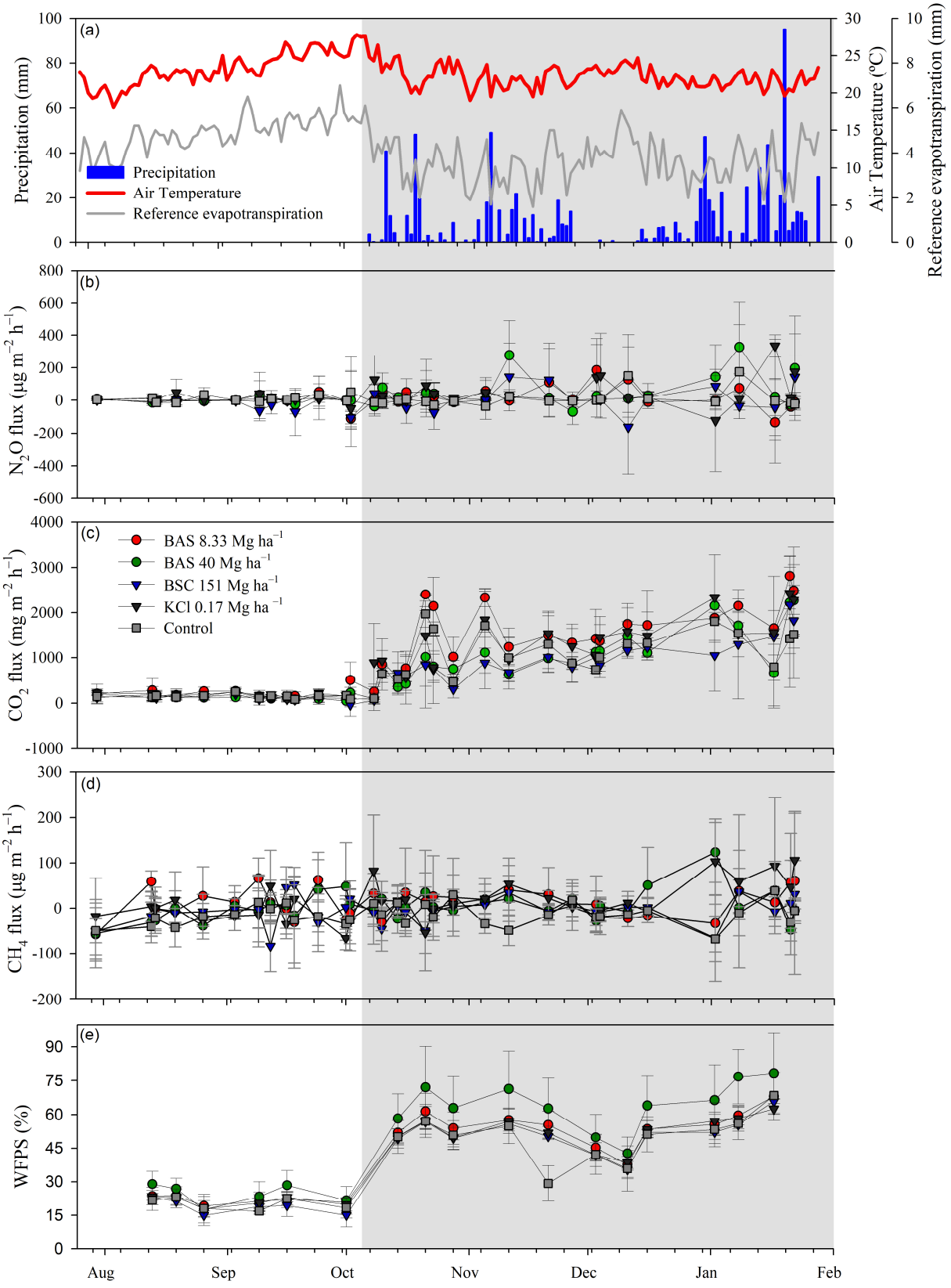

Figure 3. Total daily precipitation (mm), air temperature (°C) (**a**), soil N_2O fluxes (**b**), CO_2 (**c**), CH_4 (**d**), and daily water-filled porous space—WFPS (**e**) were recorded during the cultivation of *Urochloa brizantha* cv. BRS Paiaguás with soil remineralizers treatments in the Central Cerrado region. The shaded area refers to the rainy season. BAS: basalt; BSC: biotite schist.

Table 2. Nitrate (NO_3^-) content in soil at a depth of 0–10 cm for *Urochloa brizantha* cv. BRS Paiaguás cultivation under remineralizers application in the Central Cerrado region. BAS: basalt; BSC: biotite schist.

	BAS 8.33 Mg ha^{-1}	BAS 40 Mg ha^{-1}	BSC 151 Mg ha^{-1}	KCl 0.17 Mg ha^{-1}	Control
			NO_3^- mg kg^{-1} Soil		
13 August 2024	0.33 ± 0.04 aD	0.30 ± 0.07 aD	0.30 ± 0.060 aD	0.31 ± 0.09 aD	0.26 ± 0.08 aD
9 September 2024	0.44 ± 0.03 aC	0.43 ± 0.03 aC	0.45 ± 0.02 aC	0.47 ± 0.04 aC	0.47 ± 0.02 aC
14 October 2024	0.67 ± 0.04 aB	0.68 ± 0.05 aA	0.69 ± 0.06 aB	0.61 ± 0.07 aB	0.62 ± 0.12 aB
21 November 2024	0.53 ± 0.03 aC	0.53 ± 0.04 aC	0.51 ± 0.07 aC	0.53 ± 0.02 aBC	0.49 ± 0.04 aC
11 December 2024	0.49 ± 0.02 bC	0.52 ± 0.01 abBC	0.53 ± 0.02 aC	0.54 ± 0.02 aBC	0.53 ± 0.02 aC
17 January 2025	0.87 ± 0.05 aA	0.74 ± 0.04 bA	0.81 ± 0.02 abA	0.77 ± 0.07 abA	0.81 ± 0.09 abA

Values are presented as mean ± standard deviation. Different lowercase letters within rows and uppercase letters within columns denote statistically significant differences among treatments, as determined by Fisher's LSD test ($p < 0.05$).

The highest nitrate levels were recorded in January 2025, with concentrations of 0.87, 0.74, 0.81, 0.77, and 0.81 mg kg^{-1} observed for the treatments BAS at 8.33 Mg ha^{-1}, BAS at 40 Mg ha^{-1}, BSC at 151 Mg ha^{-1}, KCl at 0.17 Mg ha^{-1}, and the Control, respectively (Table 2). Nitrate levels were significantly affected by the treatments only in December and January ($p < 0.05$). In December, the BAS treatments did not show any differentiation between them; BAS at 8.33 Mg ha^{-1} demonstrated lower nitrate concentrations compared to BSC, KCl, and the Control treatment. In January, BAS at 40 Mg ha^{-1} resulted in lower nitrate content than at 8.33 Mg ha^{-1}, whereas no significant differences were observed among the other treatments.

The highest ammonium concentrations were observed in October 2024, with measured values of 11.84, 12.98, 9.73, 10.29, and 7.68 mg kg^{-1} for the treatments of BAS at 8.33 Mg ha^{-1}, BAS at 40 Mg ha^{-1}, BSC at 151 Mg ha^{-1}, KCl at 0.17 Mg ha^{-1}, and the Control, respectively (Table 3). In this period ammonium contents were higher than in the other periods ($p < 0.05$), except for the Control, which remained unchanged. In October, the Control treatment had less ammonium than the BAS at 40 Mg ha^{-1} treatment.

Table 3. Soil ammonium (NH_4^+) concentrations at the 0–10 cm depth under the cultivation of *Urochloa brizantha* cv. BRS Paiaguás with ASi application in the Central Cerrado region. BAS: basalt; BSC: biotite schist.

	BAS 8.33 Mg ha^{-1}	BAS 40 Mg ha^{-1}	BSC 151 Mg ha^{-1}	KCl 0.17 Mg ha^{-1}	Control
			NH_4^+ mg kg^{-1} Soil		
13 August 2024	3.42 ± 1.73 aB	3.78 ± 1.98 aB	2.78 ± 0.32 aB	2.85 ± 0.75 aB	3.33 ± 0.60 aA
9 September 2024	4.14 ± 0.95 aB	7.53 ± 5.41 aB	3.73 ± 0.18 aB	3.52 ± 0.78 aB	3.88 ± 1.12 aA
14 October 2024	11.84 ± 5.77 abA	12.98 ± 5.07 aA	9.73 ± 3.94 abA	10.29 ± 3.67 abA	7.68 ± 3.54 bA
21 November 2024	4.89 ± 0.43 aB	5.13 ± 0.63 aB	5.01 ± 2.53 aAB	5.78 ± 1.62 aAB	5.10 ± 0.50 aA
11 December 2024	4.20 ± 0.43 aB	3.44 ± 0.59 aB	3.84 ± 1.24 aB	4.11 ± 0.89 aB	3.67 ± 0.79 aA
17 January 2025	6.06 ± 1.38 aB	4.91 ± 0.83 aB	5.76 ± 1.14 aAB	4.13 ± 0.79 aB	5.36 ± 0.66 aA

Values are presented as mean ± standard deviation. Distinct lowercase letters within rows and uppercase letters within columns denote statistically significant differences among treatments, as determined by Fisher's LSD test ($p < 0.05$).

3.2. Cumulative Emissions of N_2O, CO_2, and CH_4 and Their Global Warming Potential (GWP) in Urochloa brizantha cv. BRS Paiaguás

Cumulative CO_2 emissions varied significantly ($p < 0.05$) among treatments, ranging from 2915.41 to 4338.41 kg ha^{-1}. The greatest total emissions were observed in the treatment with BAS at 8.33 Mg ha^{-1}, which showed approximately 49% higher CO_2 emissions than the treatments with higher BAS doses at 40 Mg ha^{-1} and BSC at 151 Mg ha^{-1}.

Cumulative N_2O emissions were also affected by fertilizer application ($p < 0.05$), ranging from 0.34 kg ha^{-1} with BSC at 151 Mg ha^{-1} to 1.16 kg ha^{-1} with KCl. Overall, two distinct groups emerged: KCl and BAS at 40 Mg ha^{-1} resulted in higher N_2O emissions compared to the group comprising BAS at 8.33 Mg ha^{-1}, BSC at 151 Mg ha^{-1}, and the Control treatment. Notably, KCl, a soluble potassium source, resulted in about 241% higher N_2O emissions than BSC at 151 Mg ha^{-1}. Conversely, when BSC was applied at a high dose (151 Mg ha^{-1}), a reduction in N_2O emissions was observed, likely due to the gradual release of nutrients and reduced stimulation of nitrifying microbial activity.

Cumulative CH_4 emissions ranged from –0.76 to 0.65 kg ha^{-1}. The BAS treatments showed intermediate values (0.27 and 0.47 kg ha^{-1} at 8.33 Mg ha^{-1} and 40 Mg ha^{-1}, respectively), whereas only KCl (0.65 kg ha^{-1}) produced higher CH_4 emissions than the control (Table 4). In relative terms, CH_4 emissions under KCl were about 141% higher than those observed for BAS at 8.33 Mg ha^{-1}, reinforcing the influence of the potassium source on greenhouse gas dynamics.

Table 4. Cumulative emissions of N_2O, CO_2, and CH_4 along with their respective standard deviations for *Urochloa brizantha* cv. BRS Paiaguás cultivated with remineralizers in the Central Cerrado region.

Treatment	Cumulative Emissions		
	N_2O	CO_2	CH_4
	kg ha^{-1}		
Basalt 8.33 Mg ha^{-1}	0.61 ± 0.08 b	4338.41 ± 267.92 a	0.27 ± 0.09 ab
Basalt 40 Mg ha^{-1}	1.16 ± 0.34 a	3041.18 ± 425.03 b	0.47 ± 0.33 a
Biotite schist 151 Mg ha^{-1}	0.34 ± 0.28 b	2915.41 ± 532.02 b	−0.28 ± 0.10 bc
KCl 0.17 Mg ha^{-1}	1.49 ± 0.12 a	3779.64 ± 824.47 ab	0.65 ± 0.51 a
Control	0.59 ± 0.33 b	3272.01 ± 810.16 ab	−0.76 ± 0.32 c

Values are presented as mean ± standard deviation. Distinct letters denote statistically significant differences as determined by Fisher's LSD test ($p < 0.05$).

The global warming potential (GWP) associated with the cultivation of *Urochloa brizantha* cv. BRS Paiaguás was affected by the remineralizer application ($p < 0.05$; Table 5). Treatments using KCl and BAS at 40 Mg ha^{-1} exhibited the highest GWP values, reaching 415.35 and 321.18 kg CO_2 eq. ha^{-1}, respectively. In contrast, treatments with BAS at 8.33 Mg ha^{-1}, the Control, and BSC at 151 Mg ha^{-1} showed lower values, corresponding to 138.64, 135.99, and 81.67 kg CO_2 eq. ha^{-1}, respectively.

Table 5. Global Warming Potential (GWP) values for *Urochloa brizantha* cv. BRS Paiaguás following the application of remineralizers in the Central Cerrado region.

Treatment	GWP (kg CO_2 eq. ha^{-1})
Basalt 8.33 Mg ha^{-1}	168.64 ± 21.98 b
Basalt 40 Mg ha^{-1}	321.18 ± 97.55 a
Biotite schist 151 Mg ha^{-1}	81.67 ± 74.21 b
KCl 0.17 Mg ha^{-1}	415.35 ± 28.95 a
Control	135.99 ± 82.50 b

Values are presented as mean ± standard deviation. Distinct letters denote statistically significant differences as determined by Fisher's LSD test ($p < 0.05$).

When comparing the extremes, the GWP under KCl 0.17 at Mg ha^{-1} was approximately 408% higher than that observed with BSC at 151 Mg ha^{-1}, which recorded the lowest value. Similarly, BAS at 40 Mg ha^{-1} resulted in about 294% higher GWP compared to BSC at 151 Mg ha^{-1}.

3.3. Total Carbon in the Soil

At a depth of up to 60 cm, total soil C content demonstrated no statistically significant differences ($p < 0.05$) among the treatments (Table 6). It was observed that the highest total C content was observed at soil depths of 0–10 cm and 10–20 cm, with concentrations ranging from 24.51 to 33.89 g C kg^{-1}. In contrast, the lowest concentrations were found at depths of 40–60 cm, ranging from 15.36 to 15.97 g C kg^{-1}.

Table 6. Total soil carbon content (g kg^{-1}) associated with the cultivation of *Urochloa brizantha* cv. BRS Paiaguás under remineralizers treatments in the Central Cerrado region. BAS: basalt; BSC: biotite schist.

Total Carbon (g kg^{-1} Soil)					
Depth (cm)	**BAS 8.33 Mg ha^{-1}**	**BAS 40 Mg ha^{-1}**	**BSC 151 Mg ha^{-1}**	**KCl 0.17 Mg ha^{-1}**	**Control**
0–10	32.89 ± 3.44	29.26 ± 1.64	33.88 ± 1.31	30.52 ± 0.66	31.31 ± 2.12
10–20	27.98 ± 1.13	24.51 ± 1.47	25.89 ± 1.08	25.60 ± 2.97	26.04 ± 0.96
20–30	21.35 ± 2.73	20.45 ± 1.88	19.71 ± 1.07	21.19 ± 2.00	20.85 ± 0.74
30–40	19.07 ± 0.12	17.91 ± 0.46	18.15 ± 0.66	18.28 ± 1.64	19.36 ± 1.76
40–60	15.72 ± 1.31	15.36 ± 1.81	15.47 ± 1.26	15.78 ± 0.54	15.97 ± 0.17

Values are presented as mean ± standard deviation.

3.4. Carbon and Nitrogen Stocks

Applying BAS at 8.33 Mg ha^{-1} increased soil C stocks ($p < 0.05$) in the 0–60 cm layer compared to BAS at 40 Mg ha^{-1}, while no significant differences were observed for the other treatments (Figure 4). Furthermore, BAS at 8.33 Mg ha^{-1} resulted in approximately 9.6% higher soil C stocks than BAS at 40 Mg ha^{-1}, which had the lowest value among the silicate rock treatments. No additional gains in soil C sequestration were observed with higher BAS doses, and there were no significant differences among the other treatments. The mean C stock values were 158.21, 144.35, 152.65, 153.36, and 156.80 Mg ha^{-1} for BAS at 8.33 Mg ha^{-1}, BAS at 40 Mg ha^{-1}, BSC at 151 Mg ha^{-1}, KCl at 0.17 Mg ha^{-1}, and the Control, respectively (Figure 4).

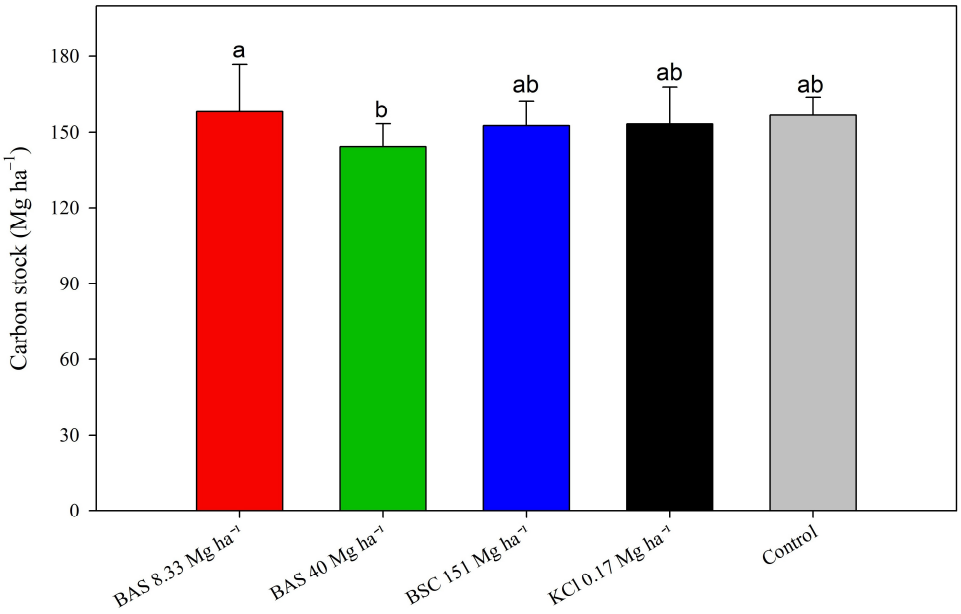

Figure 4. Soil carbon stock for *Urochloa brizantha* cv. BRS Paiaguás under different remineralizer treatments in the Central Cerrado. Bars depict mean values, with error bars representing standard deviations. BAS: basalt; BSC: biotite schist. Distinct letters denote statistically significant differences as determined by Fisher's LSD test ($p < 0.05$).

Applying BAS at 8.33 Mg ha^{-1} resulted in approximately 9.6% higher soil C stocks compared to the BAS at 40 Mg ha^{-1} treatment, which exhibited the lowest value among the remineralizer treatments. No significant differences were observed among the other treatments, indicating that higher BAS doses did not further enhance soil C sequestration.

Soil N stocks in the 0–60 cm layer were affected by treatments ($p < 0.05$; Figure 5). The highest N stock was observed in the BAS at 8.33 Mg ha^{-1} treatment, with 13.45 Mg N ha^{-1}, representing approximately 12% more N than BAS at 40 Mg ha^{-1} and about 40% more N than KCl at 0.17 Mg ha^{-1}, which showed the lowest value among the comparable treatments. The BSC at 151 Mg ha^{-1}, KCl at 0.17 Mg ha^{-1}, and Control treatments yielded similar values (10.31, 9.62, and 10.40 Mg N ha^{-1}, respectively), with no statistically significant differences among them.

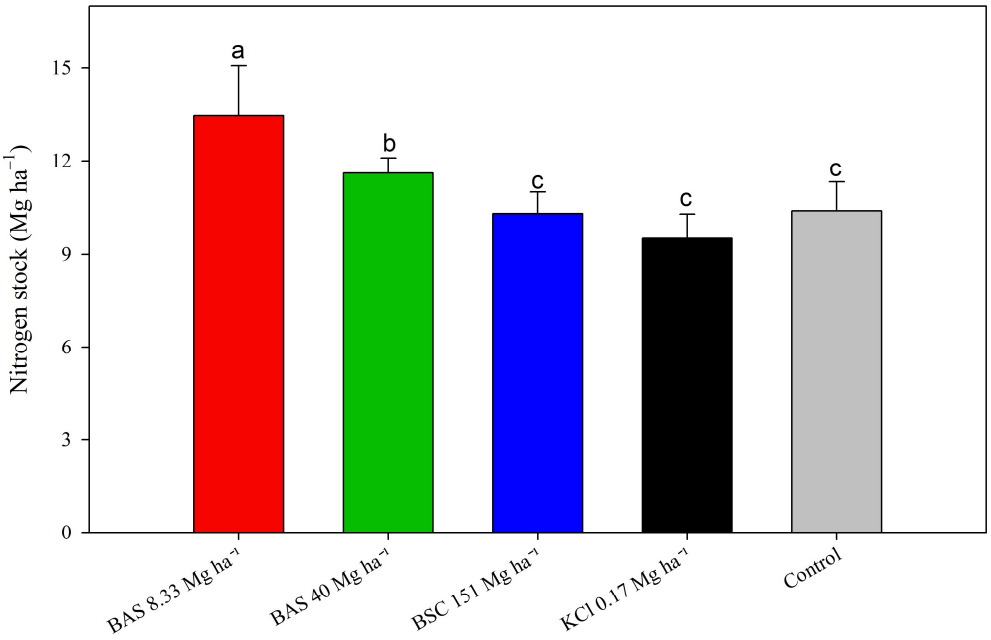

Figure 5. Soil nitrogen stock during the cultivation of *Urochloa brizantha* cv. BRS Paiaguás under remineralizer treatments in the central Cerrado region. Bars depict the mean values, with error bars representing the standard deviation. BAS: basalt; BSC: biotite schist. Distinct letters denote statistically significant differences as determined by Fisher's LSD test ($p < 0.05$).

3.5. Soil Enzymatic Activity

Soil enzymatic activity was assessed by measuring the release of p-nitrophenol resulting from the actions of arylsulfatase and β-glucosidase following application of various mineral treatments. The results showed no statistically significant differences among the treatments ($p > 0.05$). Arylsulfatase activity ranged from 64.33 µg p-nitrophenol g^{-1} soil in the KCl treatment (0.17 Mg ha^{-1}) to 83.00 µg p-nitrophenol g^{-1} soil in the BSC treatment (151 Mg ha^{-1}). The control and BAS treatments (8.3 and 40 Mg ha^{-1}) exhibited intermediate values of 70.67 and 67.00 µg p-nitrophenol g^{-1} soil, respectively. For β-glucosidase, activity levels ranged from 57.33 to 80.33 µg p-nitrophenol g^{-1} soil under the KCl 0.17 Mg ha^{-1} and Control treatments, respectively. In contrast, for the remineralizer treatments BAS at 8.33 Mg ha^{-1}, BAS at 40 Mg ha^{-1}, and BSC at 151 Mg ha^{-1}, the respective values were 77.67, 66.67, and 67.67 µg p-nitrophenol g^{-1} soil (Figure 6).

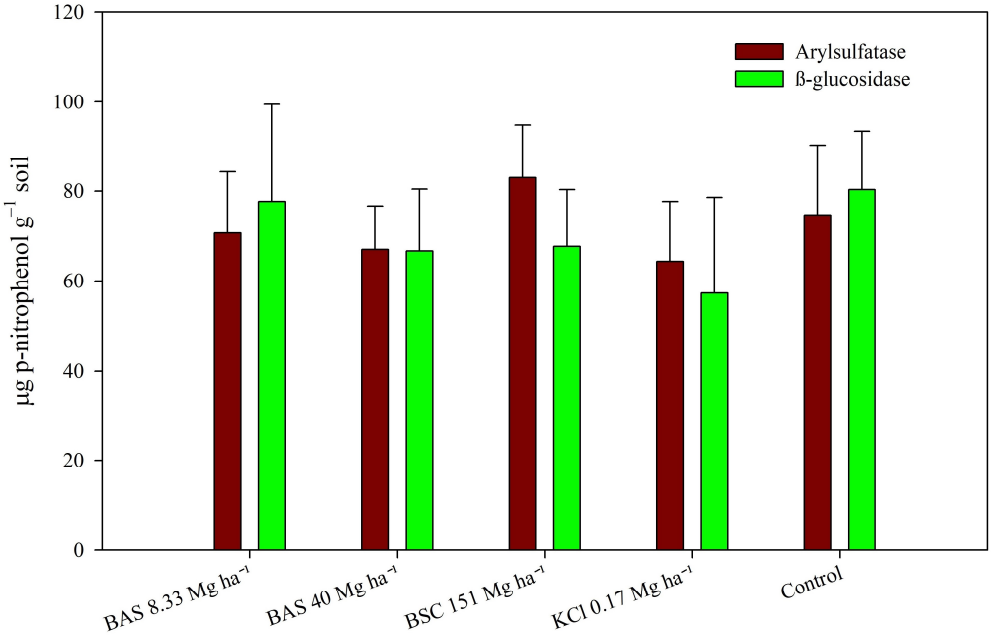

Figure 6. Enzymatic activities of arylsulfatase and β-glucosidase (µg p-nitrophenol g^{-1} soil) measured in soils subjected to various treatments. Bars depict the mean values, with error bars representing the standard deviation. Statistical analysis revealed no significant differences among treatments ($p > 0.05$). BAS: basalt; BSC: biotite schist.

The findings indicate that, within the experimental conditions assessed, mineral treatments did not result in observable changes in soil enzymatic activity.

4. Discussion

4.1. From Mineral Weathering to Nutrient Release Dynamics: Impacts on Carbon and Nitrogen Stocks and Soil Enzymatic Activity

The effects of remineralizer application on soil carbon and nitrogen accumulation and stabilization are closely linked to the mineralogy of the agrominerals used and their weathering rates and nutrient release patterns. Silicate minerals, such as those found in basalt and biotite schist, release nutrients gradually through chemical dissolution and mineral alteration, in contrast to conventional soluble sources such as KCl [19,29]. Basalt, predominantly composed of highly reactive mafic silicates, tends to supply base cations such as Ca^{2+}, Mg^{2+}, and K^{+} at relatively higher rates, whereas biotite schist consists of lamellar minerals rich in structural potassium and iron, whose dissolution is slower and strongly controlled by soil physicochemical properties and mineral–microorganism interactions [29,49,50]. This progressive nutrient release may promote more stable soil conditions over time, thereby contributing to the retention and accumulation of soil carbon and nitrogen, particularly when compared with the use of highly soluble fertilizers.

Over a nine-year period of experimentation (September 2015 to October 2024), the findings showed that none of the remineralizer treatments led to statistically significant increases in C stocks compared with the control. However, a clear dose-dependent effect was noted, with a lower dose of BAS resulting in a greater soil carbon stock than a higher dose. In this study, the lack of difference between remineralizer treatments and the no-K control highlights the challenge of increasing soil C stocks in Cerrado tropical soils. Constraints include limited management practices that add organic matter, such as cover cropping, organic amendments, or systems that increase root biomass deposition, and the Cerrado's climatic regime, which can restrict organic C accumulation rates due to alternating dry and rainy seasons. Moreover, the slow nutrient release from the remineralizer, while beneficial

for long-term sustainability, may have been insufficient over the study period to overcome these limiting factors; thus, effects on C stocks may appear only over longer timescales or may require complementary management to maximize organic matter accrual.

The results also underscore the difficulty of demonstrating atmospheric CO_2 sequestration via reactions with silicate rocks under field conditions; targeted studies isolating this process across different plant species and soil types in the Cerrado are needed. In contrast, the highest soil N stocks in this study were observed following basalt application. Basalts are among the more rapidly weathering silicate rocks [50]; their nutrient release may have improved N use efficiency, reduced losses [26] and thereby increased soil N pools. The notable impact on nitrogen levels shows that, given the experiment conditions and timeframe, applying basalt as a remineralizer effectively boosted soil nitrogen accumulation.

Furthermore, by enhancing N retention within the soil's solid phase, the availability of inorganic nitrogen species in the soil solution is reduced. With less free nitrogen available for microbial nitrification and denitrification, N_2O emissions are naturally suppressed. Consequently, basalt application modulates nitrogen partitioning, favoring organic storage over gaseous losses.

Soil enzymes are sensitive indicators of ecosystem quality and functionality, as they are directly involved in the mineralization of organic matter [51] and in the cycling of essential elements such as carbon, nitrogen, sulfur, and phosphorus [52]. Despite the importance of these enzymes, this study did not show significant differences in enzymatic activity in soils treated with silicate agrominerals. However, this apparent stability should not be interpreted as a lack of effect, but rather as a reflection of the treatments and the soil's resilience. Unlike soluble fertilizers, which cause acute responses, remineralizers are slow-release materials that promote gradual changes in soil chemistry. Enzymatic responses reflect complex signals that are modulated by environmental conditions and soil physicochemical properties. Because these activities capture only partial functional shifts within the system, enzymatic metrics must be interpreted in conjunction with broader biogeochemical and environmental indicators.

Mechanistically, this suggests that rock weathering in the dystrophic Red–Yellow Latosol is occurring at a rate that the biological system can process without causing imbalances. Because enzymatic activity serves as an early sensor of change, its stability after nearly a decade validates the system's resilience and indicates that carbon sequestration, although slow under the Cerrado climatic regime (marked by alternating dry and wet seasons), is occurring in a protected manner, without accelerating the decomposition of existing soil organic matter.

The stability of carbon stocks observed over the nine-year period may reflect a balance between cutting dynamics, which drive root-derived carbon inputs, and mineral protection mechanisms. Although nine years is a substantial duration for agricultural field trials, this timeframe constitutes a relatively short window for the complete weathering of silicates and the subsequent formation of stable organo-mineral complexes in highly weathered tropical soils.

4.2. Environmental Variables and Impact of Remineralizers on Greenhouse Gas Emissions and Global Warming Potential

The temporal dynamics of GHG emissions in this study were primarily governed by the seasonal rainfall pattern of the Cerrado (Aw climate), which directly modulated the Water-Filled Pore Space (WFPS). From October, the onset of rains, coinciding with rising soil temperatures, rewets the soil, stimulating the edaphic microbiota and thereby increasing GHG emissions to the atmosphere. The rainy season also amplifies treatment-specific responses to soil rewetting. Elevated ammonium concentrations observed in October further support increased mineralization triggered by the start of the rainy period. For

nitrate, beyond climatic influences, the higher levels recorded in January 2025 indicate a temporal pattern of nitrate accumulation.

The findings of this study suggest that silicate ASi has significant potential to reduce greenhouse gas emissions in *Urochloa brizantha* pastures in the Cerrado region. According to our findings, BSC is a promising alternative because it significantly reduces N_2O emissions and lowers the agricultural system's global warming potential (GWP). Scientific evidence indicates that applying BAS amendments is a promising approach for mitigating N_2O emissions in agricultural systems. These results indicate that using Biotite at higher application rates substantially reduces environmental impact relative to conventional fertilizers such as KCl and high-dose BAS, highlighting its potential as a sustainable alternative for mitigating global warming. Ref. [26] conducted field research involving basalt application and reported a notable decrease in cumulative N_2O emissions ranging from 29% to 32%, when basalt was incorporated into the soil during corn cultivation. These findings align with earlier research, including [27], who reported that applying basalt resulted in a 16% reduction in N_2O emissions from corn and a 9% reduction from Miscanthus. These effects were primarily attributed to increased soil pH and enhanced phosphorus availability. Furthermore, ref. [53] found that adding basaltic silicate rock dust to cattle manure not only markedly lowered NH_3 emissions but also led to a two- to threefold improvement in apparent N recovery compared with untreated manure.

Because pH did not differ among treatments, the N_2O mitigation observed with biotite addition is likely related to redox mechanisms and mineral surface interactions. Biotite alteration or dissolution releases structural Fe (II), which can supply electrons for mineral-driven autotrophic denitrification (i.e., oxidation of biotite-associated Fe (II) coupled to reduction of NO_3^-/NO_2^-). Fe(II) also participates in abiotic chemodenitrification with NO_2^-, whose outcome (increase or decrease of N_2O) depends strongly on Fe speciation, mineral surface properties and environmental conditions; thus, the net effect on N_2O production versus complete reduction to N_2 may vary between systems [49,54]. Although pH remained stable in this study, recent work shows that physicochemical soil properties, such as the ionic matrix and texture, shape denitrifier communities and the $N_2O/(N_2O+N_2)$ ratio [55]. The hypothesis that phyllosilicate surface chemistry and biotite-induced charge generation enhance this microbial pathway is plausible but requires direct experimental evidence. Overall, the results suggest that remineralizers, particularly basalt-derived materials, can contribute to carbon removal from the atmosphere while promoting CO_2 capture and reducing GHG emissions in intensive agricultural systems.

Studies conducted in crystalline aquifers demonstrate that biotite dissolution can provide electrons for autotrophic denitrification, eliminating the need for organic matter by using the released iron as an electron donor for the reduction of nitrate to N_2. [54]. This mechanism is especially relevant in tropical soils low in organic C, such as the Ferralsols of the Brazilian Cerrado, where limited organic matter can limit traditional denitrification processes.

The positive GWP values indicated that the system with *Urochloa brizantha* cv. BRS Paiaguás acted as a source of greenhouse gases (Table 5). In contrast, CH_4 functioned as a sink in the biotite schist and control treatments, whereas the remaining treatments exhibited low cumulative emissions. Thus, the contribution from N_2O emissions to GWP was greater, since CH_4 acted as a sink with negative or low values, which reduced GWP.

The higher cumulative N_2O emissions and the consequent increase in Global Warming Potential (GWP) in the KCl and high-basalt dose (BAS 40) treatments suggest a common nitrogen-loss pathway. In the case of KCl, the rapid supply of soluble potassium can alter the ionic strength of the soil solution, stimulating the mineralization of native N. For BAS 40, the massive addition of rock powder can significantly alter pH (which was not the

case in this study) and cation supply, which, although improving fertility, can accelerate nitrogen turnover during periods of high WFPS. These results highlight that remineralizer doses should be optimized to avoid negative trade-offs between soil health and climate mitigation.

In addition, the application of remineralizers, such as biotite schist and basalt, can improve soil structure and fertility by raising pH and increasing nutrient availability, which favors both plant development and the microbial activity responsible for mitigating GHG emissions [29,30]. These effects, as discussed in recent studies, reinforce the potential of remineralizers to contribute not only to sustainable soil management but also to strategies for reducing the climate impact in intensive agriculture systems.

The geochemical contrast between BAS and BSC reinforces that the use of silicate remineralizers is not a single strategy, but a targeted intervention for sustainable intensification. Our findings reveal that, while BAS strengthens soil nitrogen reservoirs, its application requires careful calibration to avoid emission peaks observed at high doses, reflecting the environmental costs of conventional KCl fertilization. On the other hand, BSC offers an efficient pathway for atmospheric mitigation, balancing N_2O suppression with the preservation of methane oxidation. This dual action, nutrient enrichment and greenhouse gas attenuation, coupled with the observed stability of soil enzymes, positions rock powder as a pillar for mineral-mediated carbon and nitrogen management. Ultimately, these results provide a roadmap for transitioning Cerrado pastures from potential carbon sources to resilient sinks, aligning agricultural productivity with low-carbon agriculture.

5. Conclusions

This study demonstrates that remineralizers derived from basalt (BAS) and biotite schist (BSC) exert distinct effects on soil nitrogen dynamics and GHG emissions. BAS (particularly at 8.33 Mg ha^{-1}) enhances soil nitrogen stocks and availability, though its climate mitigation potential is dose-dependent, as higher rates (BAS) may increase the Global Warming Potential (GWP). In contrast, BSC stands out as a superior strategy for climate-smart agriculture, significantly reducing N_2O emissions and GWP while maintaining the soil's capacity as a CH_4 sink. These findings suggest that the selection of remineralizers should be goal-oriented: BAS for enhancing fertility and nitrogen accumulation, and BSC for targeted GHG mitigation. While carbon sequestration may require longer timescales, the stability of soil enzymatic activity confirms the environmental safety of these minerals. Overall, silicate remineralizers offer a scalable and sustainable alternative to conventional fertilizers, supporting the transition to low-carbon systems in the Brazilian Cerrado.

Author Contributions: M.V.A.d.S.: formal analysis, writing—review and editing. A.D.d.O.: conceptualization, methodology, investigation, formal analysis, supervision, funding acquisition, writing—original draft, writing—review and editing. C.C.d.F.: formal analysis, writing—review and editing. J.P.G.S.: conceptualization, writing—review and editing. G.M.: writing—review and editing T.X.S.: writing—review and editing. A.C.M.d.A.: writing—review and editing. D.H.d.F.M.: chromatographic analyses. J.F.L.F.: writing—review and editing. A.M.d.C.: writing—review and editing. M.A.C.d.S.: writing—review and editing. É.d.S.M.: methodology, investigation, funding acquisition, writing—review and editing. All authors have read and agreed to the published version of the manuscript.

Funding: This research was funded through a partnership between Embrapa Cerrados and Vale S.A. (grant no. 22300.22/0199-5), and FINEP (grant number no. 1541/22).

Data Availability Statement: The data presented in this study are available on request from the corresponding author.

Acknowledgments: The authors would like to thank Vale S.A., FINEP and Embrapa Cerrados for the financial support provided for the realization of this study.

Conflicts of Interest: Authors were employed by Empresa Brasileira de Pesquisa Agropecuária and the University of Brasilia. The co-authors Marcos Vinicius Araujo dos Santos and Altair César Moreira de Andrade are interns at Embrapa Cerrados. The authors declare that the research was conducted in the absence of any commercial or financial relationships that could be construed as a potential conflict of interest.

Abbreviations

The following abbreviations are used in this manuscript:

N_2O	Nitrous Oxide
CH_4	Methane
GWP	Global warming potential
GHG	Greenhouse gas
BD	Soil bulk density
OM	Organic matter
NH_4^+	Ammonium
NO_3^-	Nitrate

References

1. Liang, X.; Yu, S.; Ju, Y.; Wang, Y.; Yin, D. Integrated Management Practices Foster Soil Health, Productivity, and Agroecosystem Resilience. *Agronomy* **2025**, *15*, 1816. [CrossRef]
2. Rehman, A.; Farooq, M.; Lee, D.-J.; Siddique, K.H.M. Sustainable Agricultural Practices for Food Security and Ecosystem Services. *Environ. Sci. Pollut. Res.* **2022**, *29*, 84076–84095. [CrossRef] [PubMed]
3. Lal, R. Farming Systems to Return Land for Nature: It's All about Soil Health and Re-Carbonization of the Terrestrial Biosphere. *Farming Syst.* **2023**, *1*, 100002. [CrossRef]
4. Crippa, M.; Solazzo, E.; Guizzardi, D.; Monforti-Ferrario, F.; Tubiello, F.N.; Leip, A. Food Systems Are Responsible for a Third of Global Anthropogenic GHG Emissions. *Nat. Food* **2021**, *2*, 198–209. [CrossRef]
5. Boakes, E.H.; Dalin, C.; Etard, A.; Newbold, T. Impacts of the Global Food System on Terrestrial Biodiversity from Land Use and Climate Change. *Nat. Commun.* **2024**, *15*, 5750. [CrossRef]
6. SEEG—Sistema de Estimativas de Emissões e Remoções de Gases de Efeito Estufa. Available online: https://plataforma.seeg.eco.br/ (accessed on 27 June 2025).
7. LAPIG. Available online: https://atlasdaspastagens.ufg.br (accessed on 3 July 2025).
8. Bieluczyk, W.; Cherubin, M.R.; Cerri, C.E.P.; Siqueira-Neto, M.; Abdalla-Filho, A.L.; Castro, J.I.A.; Locatelli, J.L.; Tsai, S.M.; de Camargo, P.B. Greenhouse Gas Fluxes in Brazilian Climate-Smart Agricultural and Livestock Systems: A Systematic and Critical Overview. *J. Clean. Prod.* **2024**, *464*, 142782. [CrossRef]
9. Ramos, M.L.G.; da Costa, A.R.; Madari, B.E.; Carvalho, G.D.; Pereira, A.C.d.C.; Corrêa, R.S.; de Sousa, T.R.; de Carvalho, A.M. Nitrous Oxide Emissions and Ammonia Volatilization from Pasture after Cattle Dung and Urine Applications in the Dry and Rainy Seasons of the Brazilian Cerrado. *Agronomy* **2024**, *14*, 1257. [CrossRef]
10. de Oliveira, A.D.; Ribeiro, F.P.; de Figueiredo, C.C.; Muller, A.G.; Vitoria Malaquias, J.; dos Santos, I.L.; de Sá, M.A.C.; Soares, J.P.G.; dos Santos, M.V.A.; de Carvalho, A.M. Effects of Soil Management, Rotation and Sequence of Crops on Soil Nitrous Oxide Emissions in the Cerrado: A Multi-Factor Assessment. *J. Environ. Manag.* **2023**, *348*, 119295. [CrossRef]
11. Rodrigues, C.I.D.; Brito, L.M.; Nunes, L.J.R. Soil Carbon Sequestration in the Context of Climate Change Mitigation: A Review. *Soil Syst.* **2023**, *7*, 64. [CrossRef]
12. Manning, D.A.C.; Baptista, J.; Sanchez Limon, M.; Brandt, K. Testing the Ability of Plants to Access Potassium from Framework Silicate Minerals. *Sci. Total Environ.* **2017**, *574*, 476–481. [CrossRef]
13. Segnini, A.; Xavier, A.A.P.; Otaviani-Junior, P.L.; Oliveira, P.P.A.; Pedroso, A.d.F.; Praes, M.F.F.M.; Rodrigues, P.H.M.; Milori, D.M.B.P. Soil Carbon Stock and Humification in Pastures under Different Levels of Intensification in Brazil. *Sci. Agric.* **2019**, *76*, 33–40. [CrossRef]
14. Fronza, E.E.; Caten, A.T.; Bittencourt, F.; Zambiazi, D.C.; Filho, A.L.S.; Seó, H.L.S.; Loss, A. Carbon Sequestration Potential of Pastures in Southern Brazil: A Systematic Review. *Rev. Bras. Ciênc. Solo* **2024**, *48*, e0230121. [CrossRef]
15. Zaman, K. Environmental Cost of Deforestation in Brazil's Amazon Rainforest: Controlling Biocapacity Deficit and Renewable Wastes for Conserving Forest Resources. *For. Ecol. Manag.* **2022**, *504*, 119854. [CrossRef]
16. Oosting, S.; van der Lee, J.; Verdegem, M.; de Vries, M.; Vernooij, A.; Bonilla-Cedrez, C.; Kabir, K. Farmed Animal Production in Tropical Circular Food Systems. *Food Secur.* **2022**, *14*, 273–292. [CrossRef]

17. Kamyab, H.; SaberiKamarposhti, M.; Hashim, H.; Yusuf, M. Carbon Dynamics in Agricultural Greenhouse Gas Emissions and Removals: A Comprehensive Review. *Carbon Lett.* **2024**, *34*, 265–289. [CrossRef]
18. de Abreu Lima, R.C.; Lemos, F.K. Brazilian Agriculture and the Global Environmental Agenda. In *Sustainability Challenges of Brazilian Agriculture: Governance, Inclusion, and Innovation*; Søndergaard, N., de Sá, C.D., Barros-Platiau, A.F., Eds.; Springer International Publishing: Cham, Switzerland, 2023; pp. 85–105, ISBN 978-3-031-29853-0.
19. Basak, B.B.; Sarkar, B.; Naidu, R. Environmentally Safe Release of Plant Available Potassium and Micronutrients from Organically Amended Rock Mineral Powder. *Environ. Geochem. Health* **2021**, *43*, 3273–3286. [CrossRef]
20. Rodrigues, L.N.F.; Borges, W.L.B.; Modesto, V.C.; Ribeiro, N.A.A.; de Souza, N.C.; Girardi, V.A.M.; Matos, A.M.S.; Silva, B.P.C.; Galindo, F.S.; Andreotti, M. Use of Soil Remineralizer to Replace Conventional Fertilizers: Effects on Soil Fertility, Enzymatic Parameters, and Soybean and Sorghum Productivity. *Agriculture* **2024**, *14*, 2153. [CrossRef]
21. Biswas, S.; Singh, S.; Bera, A. Regenerative Nutrient Management Practices for Enhancing Plant Nutrition and Soil Health. In *Regenerative Agriculture for Sustainable Food Systems*; Kumar, S., Meena, R.S., Sheoran, P., Jhariya, M.K., Eds.; Springer Nature: Singapore, 2024; pp. 303–339, ISBN 978-981-97-6691-8.
22. Palma, H.H.; Granados, A.I.N.; Neckel, A.; Osorio, D.P.; Ríos, A.L.M.; Ramos, C.G. Valorization of Mineral By-Products through Soil Remineralization Enhances Sustainable Agriculture and Circular Economy Outcomes. *Discov. Sustain.* **2025**, *6*, 1134. [CrossRef]
23. Cardozo, E.S.; Alves, J.B.; Pinto, V.; Nadaleti, W.; Thue, P.S.; dos Santos, M.C.; Michelin, C.; Gomes, C.G.; Ribeiro, A.S.; Machado, J.B.; et al. Geological Viability and Nutrient Availability of Andesitic Basalt Rock Powder as a Soil Remineralizer. *Discov. Geosci.* **2025**, *3*, 134. [CrossRef]
24. Luchese, A.V.; Gutz de Castro Leite, I.J.; da Silva Giaretta, A.P.; Alves, M.L.; Pivetta, L.A.; Missio, R.F. Use of Quarry Waste Basalt Rock Powder as a Soil Remineralizer to Grow Soybean and Maize. *Heliyon* **2023**, *9*, e14050. [CrossRef]
25. Rosalen, K.; Baretta, D.; Baretta, C.R.D.M.; Oliveira Filho, L.C.L.; Galina, J.; Golin, Í.L. Effect of Remineralizer on Soil Biological Quality. *Biologia* **2024**, *79*, 3327–3336. [CrossRef]
26. Chiaravalloti, I.; Theunissen, N.; Zhang, S.; Wang, J.; Sun, F.; Ahmed, A.A.; Pihlap, E.; Reinhard, C.T.; Planavsky, N.J. Mitigation of Soil Nitrous Oxide Emissions during Maize Production with Basalt Amendments. *Front. Clim.* **2023**, *5*, 43. [CrossRef]
27. Blanc-Betes, E.; Kantola, I.B.; Gomez-Casanovas, N.; Hartman, M.D.; Parton, W.J.; Lewis, A.L.; Beerling, D.J.; DeLucia, E.H. In Silico Assessment of the Potential of Basalt Amendments to Reduce N_2O Emissions from Bioenergy Crops. *GCB Bioenergy* **2021**, *13*, 224–241. [CrossRef]
28. Weber, J.; Keeble, J.; Abraham, N.L.; Beerling, D.J.; Martin, M.V. Global Agricultural N_2O Emission Reduction Strategies Deliver Climate Benefits with Minimal Impact on Stratospheric O_3 Recovery. *npj Clim. Atmos. Sci.* **2024**, *7*, 121. [CrossRef]
29. Swoboda, P.; Döring, T.F.; Hamer, M. Remineralizing Soils? The Agricultural Usage of Silicate Rock Powders: A Review. *Sci. Total Environ.* **2022**, *807*, 150976. [CrossRef]
30. Beerling, D.J.; Leake, J.R.; Long, S.P.; Scholes, J.D.; Ton, J.; Nelson, P.N.; Bird, M.; Kantzas, E.; Taylor, L.L.; Sarkar, B.; et al. Farming with Crops and Rocks to Address Global Climate, Food and Soil Security. *Nat. Plants* **2018**, *4*, 138–147. [CrossRef]
31. Alvares, C.A.; Stape, J.L.; Sentelhas, P.C.; de Moraes Gonçalves, J.L.; Sparovek, G. Köppen's Climate Classification Map for Brazil. *Meteorol. Z.* **2013**, *22*, 711–728. [CrossRef]
32. Reatto, A.; Martins, E.d.S.; Farias, M.F.R.; Silva, A.V.d.; Carvalho Júnior, O.A.d. *Mapa Pedológico Digital: SIG Atualizado do Distrito Federal Escala 1:100.000 e uma Síntese do Texto Explicativo*; Embrapa Cerrados: Planaltina, Brazil, 2004.
33. Santos, H.G.d.; Jacomine, P.K.T.; Anjos, L.H.C.d.; Oliveira, V.A.d.; Lumbreras, J.F.; Coelho, M.R.; Almeida, J.A.D.; Araujo Filho, J.C.D.; Oliveira, J.B.D.; Cunha, T.J.F. *Sistema Brasileiro de Classificação de Solos*; Embrapa: Brasília, Brazil, 2018; ISBN 978-85-7035-817-2.
34. *World Reference Base for Soil Resources 2022: International Soil Classification System for Naming Soils and Creating Legends for Soil Maps*, 4th ed.; International Union of Soil Sciences: Vienna, Austria, 2022; ISBN 979-8-9862451-1-9.
35. Teixeira, P.C.; Donagemma, G.K.; Fontana, A.; Teixeira, W.G.; Paulo Cesar Teixeira, C.G.K.D. *Manual de Métodos de Análise de Solo*; Embrapa: Brasília, Brazil, 2017; ISBN 978-85-7035-771-7.
36. Sousa, D.M.G.d.; Lobato, E. *Cerrado: Correção do Solo e Adubação*; Embrapa Informação Tecnológica: Brasília, Brazil; Embrapa Cerrados: Planaltina, Brazil, 2004; ISBN 978-85-7383-230-3.
37. Walkley, A.J.; Black, I.A. Estimation of Soil Organic Carbon by the Chromic Acid Titration Method. *Soil Sci.* **1934**, *37*, 29–38.
38. Silva, P.B.d.; Carvalho, A.M.d.; Junqueira, A.M.R.; Soares, J.P.G.; Sá, M.A.C.d.; Marchi, G.; Martins, E.d.S.; Figueiredo, C.C.d.; Santos, L.F.d.; Sousa, T.R.d.; et al. Soil Carbon and Nitrogen in Silicate Agromineral-Managed Pasture: A Seven-Year Study in the Cerrado. *Pesqui. Agropecuária Bras.* **2025**, *60*, e04133. [CrossRef]
39. Hutchinson, G.l.; Livingston, G.P. Use of Chamber Systems to Measure Trace Gas Fluxes. In *Agricultural Ecosystem Effects on Trace Gases and Global Climate Change*; John Wiley & Sons, Ltd.: Hoboken, NJ, USA, 1993; pp. 63–78, ISBN 978-0-89118-321-1.
40. Zanatta, J.A.; Alves, B.J.R.; Bayer, C.; Tomazi, M. *Protocolo Para Medição de Fluxos de Gases de Efeito Estufa do Solo*; Embrapa Florestas: Colombo, Sri Lanka, 2014; 81p.

41. Oliveira, A.D.d.; Antonini, J.C.d.A.; Santos, M.V.A.d.; Andrade, A.C.M.d.; Malaquias, J.V.; Carvalho, A.M.d.; Muller, A.G.; Delvico, F.M.d.S.; Mendes, I.d.C.; Chagas, J.H.; et al. Sustainable Irrigation Management of Winter Wheat and Effects on Soil Gas Emissions (N_2O and CH_4) and Enzymatic Activity in the Brazilian Savannah. *Sustainability* **2025**, *17*, 7734. [CrossRef]
42. Abubakar, S.A.; Hamani, A.K.M.; Chen, J.; Sun, W.; Wang, G.; Gao, Y.; Duan, A. Optimizing N-Fertigation Scheduling Maintains Yield and Mitigates Global Warming Potential of Winter Wheat Field in North China Plain. *J. Clean. Prod.* **2022**, *357*, 131906. [CrossRef]
43. Steudler, P.A.; Bowden, R.D.; Melillo, J.M.; Aber, J.D. Influence of Nitrogen Fertilization on Methane Uptake in Temperate Forest Soils. *Nature* **1989**, *341*, 314–316. [CrossRef]
44. Blake, G.R.; Hartge, K.H. Bulk Density. In *Methods of Soil Analysis*; ASA-SSSA: Madison, WI, USA, 1986; pp. 363–3982.
45. de Sousa, T.R.; de Carvalho, A.M.; Ramos, M.L.G.; de Oliveira, A.D.; de Jesus, D.R.; da Fonseca, A.C.P.; da Costa Silva, F.R.; Delvico, F.M.D.S.; Junior, F.B.D.R.; Marchão, R.L. Dynamics of Carbon and Soil Enzyme Activities under Arabica Coffee Intercropped with Brachiaria Decumbens in the Brazilian Cerrado. *Plants* **2024**, *13*, 835. [CrossRef] [PubMed]
46. Tabatabai, M.A. Soil Enzymes. In *Methods of Soil Analysis*; John Wiley & Sons, Ltd.: Hoboken, NJ, USA, 1994; pp. 775–833, ISBN 978-0-89118-865-0.
47. Diniz, A.R.; Silva, C.F.d.; Pereira, M.G.; Balieiro, F.C.; Silva, E.V.d.; Santos, F.M.d. Microbial Biomass and Enzyme Activity of Soil Under Clonal Rubber Tree Plantations. *Floresta Ambiente* **2020**, *27*, e20171138. [CrossRef]
48. Guo, D.; Ou, Y.; Zhou, X.; Wang, X.; Zhao, Y.; Li, J.; Xiao, J.; Hao, Z.; Wang, K. Response of Soil Enzyme Activities to Natural Vegetation Restorations and Plantation Schemes in a Landslide-Prone Region. *Forests* **2022**, *13*, 880. [CrossRef]
49. Murakami, T.; Utsunomiya, S.; Yokoyama, T.; Kasama, T. Biotite Dissolution Processes and Mechanisms in the Laboratory and in Nature: Early Stage Weathering Environment and Vermiculitization. *Am. Mineral.* **2003**, *88*, 377–386. [CrossRef]
50. Kantola, I.B.; Masters, M.D.; Beerling, D.J.; Long, S.P.; DeLucia, E.H. Potential of Global Croplands and Bioenergy Crops for Climate Change Mitigation through Deployment for Enhanced Weathering. *Biol. Lett.* **2017**, *13*, 20160714. [CrossRef]
51. Mendes, I.C.; Sousa, D.M.G.; Dantas, O.D.; Lopes, A.A.C.; Reis, F.B., Jr.; Oliveira, M.I.; Chaer, G.M. Soil Quality and Grain Yield. *Geoderma* **2021**, *388*, 114880.
52. Wang, L.; Hamel, C.; Lu, P.; Wang, J.; Sun, D.; Wang, Y.; Lee, S.-J.; Gan, G.Y. Using Enzyme Activities as an Indicator of Soil Fertility in Grassland—An Academic Dilemma. *Front. Plant Sci.* **2023**, *14*, 1175946. [CrossRef]
53. Swoboda, P.; Hamer, M.; Stotter, M.; Döring, T.F.; Trimborn, M. Effects of Rock Powder Additions to Cattle Slurry on Ammonia and Greenhouse Gas Emissions. *Atmosphere* **2021**, *12*, 1652. [CrossRef]
54. Roques, C.; Aquilina, L.; Boisson, A.; Vergnaud-Ayraud, V.; Labasque, T.; Longuevergne, L.; Laurencelle, M.; Dufresne, A.; de Dreuzy, J.-R.; Pauwels, H.; et al. Autotrophic Denitrification Supported by Biotite Dissolution in Crystalline Aquifers: (2) Transient Mixing and Denitrification Dynamic during Long-Term Pumping. *Sci. Total Environ.* **2018**, *619–620*, 491–503. [CrossRef]
55. Bano, S.; Wu, Q.; Yu, S.; Wang, X.; Zhang, X. Soil Properties Drive Nitrous Oxide Accumulation Patterns by Shaping Denitrifying Bacteriomes. *Environ. Microbiome* **2024**, *19*, 94. [CrossRef]